BNL--32110

DE83 003724

BNL-32110

Conf-8206116--8

October 22, 1982

Phenomenological Consequences of Supersymmetry

Ian Hinchliffe and L. Littenberg

PHENOMENOLOGICAL CONSEQUENCES OF SUPERSYMMETRY

Ian Hinchliffe

Lawrence Berkeley Laboratory
University of California
Berkeley, California 94720

L. Littenberg

Brookhaven National Laboratory
Upton, Long Island, NY 11973

BNL-32110

0. Introduction

This report deals with the phenomenological consequences of supersymmetric theories, and with the implications of such theories for future high energy machines. The report represents the work of a subgroup at the meeting. Many attendees contributed, but those primarily responsible for this report are B. Blumenfeld, D. Garelick, M. Longo, J. Leveille, R. Lipton, J. Wiss, and the two authors. Where no attribution of a calculation or figure is given it may be assumed that one of the authors is responsible for it. We will be concerned only with high energy predictions of supersymmetry; low energy consequences (for example in the $K_o\bar{K}_o$ system) are discussed in the context of future experiments by another group,[0.1] and will be mentioned briefly only in the context of constraining existing models. However a brief section is included on the implication for proton decay, although detailed experimental questions are not discussed.

The report is organized as follows. Section I consists of a brief review of supersymmetry and the salient features of existing supersymmetric models; this section can be ignored by those familiar with such models since it contains nothing new. Section 2 deals with the consequences for nucleon decay of SUSY. The remaining sections then discuss the physics possibilities of various machines; $e\bar{e}$ in Section 3, ep in Section 4, pp(or $p\bar{p}$) colliders in Section 5 and fixed target hadron machines in Section 6. Reports of earlier meetings discussing the phenomenological consequences of supersymmetry exist[0.2, 0.3] but one of these contains a number of errors[0.2] and the other restricts itself to physics on the Z^o.[0.3] In addition much progress has been made in the last year or so in model building, and the information gleaned has rendered some of the earlier assumptions invalid.

References

0.1. R. Shrock, these proceedings.
0.2. G. Barbiellini, et al., Supersymmetry at LEP, DESY report 79/67 (1979).
0.3. G. Farrar in "Proceedings of the Cornell Z^o Workshop" CLNS 81-485 (1981).

I. Supersymmetry and supersymmetric models.

Supersymmetry is a symmetry which relates fermions to bosons. Supersymmetric models have equal numbers of fermionic and bosonic degrees of freedom. The simplest such model[1.1] consists of two real scalar fields (two degrees of freedom) interacting with a Majorana fermion of the same mass (also two degrees of freedom). It has only one (logarithmic) divergence in pertubation theory, the common wave function renormalization of all three fields, whereas the most general theory involving these particles has fifteen divergences, some of which (the scalar masses) are quadratic. Supersymmetry relates coupling constants and masses, and hence reduces the number of arbitrary parameters in a Lagrangian. This powerful aesthetic argument is one reason why theorists are so excited about supersymmetry. There are two other reasons. Firstly supersymmetric theories offer a hope of being able to include gravity in a sensible manner,[1.2] and they may offer a solution to the hierarchy problem in grand unified theories. This latter hope is a primary reason for the recent upsurge in theoretical activity so we will discuss it briefly.

In a conventional grand unified theory such as SU(5),[1.3] there are two widely disparate mass scales, the scale characterizing weak interactions ($\sim 10^2$ GeV), and that characterizing the unification or the nucleon lifetime ($\sim 10^{14}$GeV). These scales appear in the Lagrangian as mass parameters for scalar fields (Higgs), and these mass parameters have quadratic divergences in perturbation theory. The difference in mass scales of some eleven orders of magnitude tends to be destroyed by higher order corrections; it is therefore necessary to adjust parameters to eleven significant figures at each order of perturbation theory. This fine tuning is unnatural;[1.4] it would be better if we could find some property of the theory, such as a symmetry, which either explained the hierarchy or removed the need for adjustment at each order of pertubation theory. For example, fermion masses can be kept zero (small) by imposing an exact (approximate) chiral symmetry on the Lagrangian. A fermion mass, if small at tree level, will tend to stay small because of this approximate symmetry. Supersymmetry affords the possibility of solving the hierarchy problem. Suppose the Lagrangian has the mass scale (M_x) and an exact supersymmetry. It is a consequence of the remarkable renormalization properties of supersymmetric theories[1.5] that any particle which has no mass in the (tree level) Lagrangian will stay massless to all orders of perturbation theory. If we now break the supersymmetry at a scale M_s (i.e. fermions and bosons become split in mass by an amount $\lesssim O(M_s)$), finite masses $\lesssim O(M_s)$ will be generated for particles which were previously massless. It is possible to arrange things so that one of these particles is the Weinberg-Salam Higgs, which obtains a negative mass of order 100 GeV. The scale M_s is stable with respect to higher orders in perturbation theory, consequently

the scales connected to it (M_W) are held small, and the hierarchy problem is solved. Of course, it must be explained why the supersymmetry breaking scale in the matter sector of the theory is so much smaller than M_X.

After this motivation we now list the particles predicted by supersymmetry and discuss their interactions. The models discussed here have only one supersymmetry (N = 1); consequently only one set of bosons and one set of fermions are related by a supersymmetry and form a supermultiplet. Higher supersymmetries exist where mutiplets contain more particles than this (e.g. spin 0, spin 1/2, and spin 1) but it seems to be impossible to use them to construct phenomenologically viable models. A chiral multiplet consists of a spin 1/2 fermion of definite chirality (e.g. e_L) with two degrees of freedom (e_L and $\bar{e}_L$) and a complex scalar ($\tilde{e}_L$) also with two degrees of freedom. Thus a Dirac fermion, for example the electron, (e_L plus e_R) has two scalars ($\tilde{e}_L$ and $\tilde{e}_R$) accompanying it. These fermions and scalars have identical quantum numbers except for spin, and are degenerate in mass in the limit of exact supersymmetry. When supersymmetry is broken, as it must be since there is no scalar degenerate with the electron, the mass eigenstates of the scalars depend on the details of the particular model, they are not necessarily $\tilde{e}_L$ and $\tilde{e}_R$. A massless spin 1 gauge field (e.g. the photon) is in a vector supermultiplet with a spin 1/2 Majorana fermion (the photino). Some convenient notation is as follows; the partner of an existing particle is denoted by adding a ~ over the top of the particle name; if the existing particle is a boson, its pertner's name is obtained by changing the ending of its name to ino, if it is a fermion, its bosonic partner is named by adding an s. Hence photon (γ) and photino ($\tilde{\gamma}$), muon (μ) and smuon ($\tilde{\mu}$). The minimal set of particles present in the supersymmetric version of the standard model can now be writtan down with two exceptions.

If the supersymmetry is broken spontaneously a massless fermion appears in the spectrum; this is analogous to a Goldstone boson which arises from the spontaneous breakdown of a bosonic symmetry, and is called a Goldstino ($\tilde{G}$). In gauge models with a bosonic symmetry (e.g. the Weinberg-Salam model), no massless scalar appears, the Goldstone boson is eaten by the gauge particle when it acquires a mass. If the supersymmetric model is coupled to gravity, a similar phenomenon can occur. The $\tilde{G}$ is eaten by the spin 3/2 partner of the graviton and acquires a mass $\sim M_s^2/M_p$ where M_p is the Planck mass[1.6] ($\sim 10^{19}$GeV); thus if M_s is small, $\tilde{G}$ is effectively massless. Unfortunately this naive coupling leads to a non-renormalizable theory, so it is not clear how meaningful this is.

The second exception is that the Higgs sector must be slightly more complicated than the minimal Weinberg-Salam model.[1.7] In this model one Higgs field (H) gives mass to the up and down quarks, when it acquires a vacuum expectation value, via Yukawa terms in the potential of the form $H\,\bar{u}_L u_R$ and $H^*\,\bar{d}_L d_R$. In a supersymmetric model both H and its complex conjugate H^* cannot appear in the superpotential. Hence we must have two Higgs doublets (H and H') in order to give mass to both u and d. The supersymmetric Weinberg-Salam model therefore requires physical, charged Higgs fields not present in the usual model. The phenomenological consequences of these Higgs scalars are discussed elsewhere[1.8]. The physical states in an SU(3) × SU(2) × U(1) supersymmetry model are listed in Table 1.

	SU(3) rep.	SU(2) rep.	Q_{em}	spin
quarks	3	2,1	2/3,-1/3	1/2
squarks	3	2,1	2/3,-1/3	0
leptons	1	2,1	1,0	1/2
sleptons	1	2,1	1,0	0
gluons	8	1	0	1
gluinos	8	1	0	1/2
photon	1	1	0	1
photino	1	1	0	1/2
W,Z	1	3	±1,0	1
Wino Zino	1	3	±1,0	1/2
Higgs	1	2	±1,0	0
Higgaino	1	2	±1,0	1/2
Goldstino	1	1	0	1/2

Table 1. Minimal set of particles in a supersymmetry SU(3) × SU(2) × U(1) model.

It is now necessary to discuss the breaking of supersymmetry and the four distinct types of phenomenological models which result.

1) Softly broken models.[1.9] In these models the supersymmetry is broken explictly by adding mass terms for the scalars in chiral multiplets ($\tilde{e}, \tilde{q}$ etc.) and for gauge fermions ($\tilde{g}, \tilde{\gamma}$ etc.). There is no natural relationship between masses in these models and, generally speaking, parameters must be carefully chosen to avoid phenomenological disasters such as flavor changing neutral currents or large parity violation. These models have no Goldstino, and have no need of more particles than the minimal set of Table 1 (plus, of course, any extra gauge and Higgs particles if the model is grand unified). Aesthetically, models of this type are somewhat unappealing. Recently models of N = 1 supersymmetry coupled to supergravity have been discussed,[1.10] they have a similar mass spectrum to the softly broken models except that all the squarks and sleptons are degenerate. Such models are not renormalizable so it is not clear how seriously they should be taken.

2) Models with spontaneous breaking of supersymmetry where squark and slepton masses appear at lowest order.[1.11] These models require that the gauge group of the Weinberg-Salam model be extended to contain at least one other U(1) factor. This means that the low energy phenomenology is changed (there are two Z's), but parameters can be adjusted[1.12] so that these models are not excluded. The minimal set of particles now also includes one extra Z (the zum) and its fermionic partner (Zumino). In addition, renormalizable models of this type have extra fields whose masses are essentially arbitrary. For example, the model of Ref. 1.13 has a color octet fermion and scalar at about 1 TeV. The negative mass for the Higgs scalars appears at tree level, consequently the mass scale associated with them is the same order as M_s; hence M_s is of order 1 TeV or less, so that the Goldstino is extremely light (assuming, of course, the formula $M_{\tilde{G}} = M_s^2/M_p$ is correct). The physical make-up of the Goldstino is model dependent, it is usually a linear combination of the Zumino and other particles. The W mass appears at the same order as the squark and slepton masses which are therefore of order M_W. It is natural, although not strictly necessary for the squarks and sleptons to be almost degenerate, the differences being

of order quark and lepton masses ($m^2_{\tilde{q},\tilde{e}} = M^2 + m^2_{q,e}$, with M being a universal number of order M_W). In these models the gluinos and photinos get mass via radiative corrections and tend to be light, a few GeV for $\tilde{g}$ and a few MeV for $\tilde{\gamma}$. The winos combine with the Higgsinos to form Dirac particles with masses of order M_W; radiative masses for the winos are too small (O(1) GeV) to be acceptable.

3) Models where the supersymmetry is spontaneously broken and the squarks and sleptons get mass via radiative corrections.[1.14,1.15] In these models a sector is added to the theory, which describes the interaction of new set of particles. Supersymmetry is broken spontaneously in this sector on scale M_s and hence the Goldstino is a linear combination of these exotic particles. This sector then communicates the supersymmetry breaking to the rest of the world via radiative corrections. As an example consider the following scenario. The extra sector contains a colored boson A and its fermionic partner ψ_A which have masses M and M + Δ respectively, where Δ is of order M_s. The squarks can couple to A and ψ_A via gluons (Fig. 1.1) and a squark mass ($m_{\tilde{q}}$) can be generated $m^2_{\tilde{q}} \approx \alpha_s^2 \Delta^2 (\frac{\Delta^2}{M^2})$.

Figure 1.1

If A and ψ_A couple to $SU(2)_{weak}$ then similar diagrams involving W's will give masses to sleptons and Higgs. It is possible to arrange these and other diagrams to produce a negative Higgs mass and then break the Weinberg-Salam symmetry.[1.14] A similar relationship to the one above then relates Δ, M, α_{em} and M_W. These models have two mass scales M_s and M, and M_s is rather weakly constrained: $M_s \gtrsim O(10$ TeV). The mass of the Goldstino is essentially arbitrary. The mechanism for generating squark masses is flavor blind so all squarks are degenerate in mass (up to quark masses). Sleptons are lighter than squarks ($\frac{m^2_{\tilde{\ell}}}{m^2_{\tilde{q}}} \approx O(\frac{\alpha^2_{em}}{\alpha^2_s})$), and since W bosons are involved in generating mass, $\tilde{e}_L$ and $\tilde{e}_R$ are not degenerate, the mass difference is of the same order as the mass itself. But again $\tilde{\nu}_L \tilde{e}_L$ and $\tilde{e}_L$ are almost degenerate. Gluinos, photinos and winos get mass via radiative corrections. Whether the gluino is lighter than the squark is a model dependent question, but in most models it tends to be so. (For an exception see ref. 1.16).

4) Supercolor models.[1.17] In these models supersymmetry is assumed to break dynamically due to the formation of some chiral condensate. There are arguments against this scenario,[1.18] and models of this type are difficult to calculate with. Their predictions for masses of squarks gluinos etc. are very model dependent. $M_s \gtrsim 10$ TeV in these models.

Despite all this ambiguity in, and the proliferation of, models it is important to stress the model independent features of supersymmetry. The interactions of squarks, sleptons, gluinos etc. are almost completely determined; they are the same as those of quarks and leptons. For example the three gluon vertex in QCD has the same strength as the two gluino–one gluon vertex. The primary ambiguity is that the masses of the supersymmetry partners are unknown. In almost all models there is a quantum number (twiddleness) which is conserved in all interactions. Hence a supersymmetric partner must always decay into another supersymmetric partner; eg $\tilde{g} \to q + \tilde{q}$ and $\tilde{e} \to e + \tilde{\gamma}$ are allowed but $\tilde{e} \to e + \nu$ is not. The only interaction of the supersymmetric partners which is not determined is the coupling to the Goldstino, which depends on the scale M_s. The coupling of $\tilde{G}$ to a particle super-particle pair (eg $\tilde{\gamma} \to \gamma + \tilde{G}$) depends on $\frac{\Delta_m}{M_s}$ where Δ_m is the mass difference between the particle and its partner (here $m_{\tilde{\gamma}}$). In particular the lifetime of the photino due to $\tilde{\gamma} \to \gamma + \tilde{G}$ is

$$\tau = 8\pi M_s^4 / (M_{\tilde{\gamma}})^5 .^*$$

The principal decay modes of supersymmetric particles are listed below. Generally speaking modes without Goldstinos dominate unless they are excluded by phase space. The lifetimes quoted are the inverse widths for that particular channel; all masses are in GeV. Some particles (e.g., $\tilde{g}$) may live long enough to leave a track (or gap) simplifying their detection. Others, if they are light (e.g., $\tilde{\gamma}$), are likely to exit the detector before decaying or interacting.

Particle	Decay mode	Lifetime (approx) sec
$\tilde{e}$	$e + \tilde{\gamma}$	$2\times10^{-22} \frac{m^3_{\tilde{e}}}{(m^2_{\tilde{e}} - m^2_{\tilde{\gamma}})^2}$
	$e + \tilde{G}$	$7\times10^{-16} (\frac{M_s}{M_W})^4 \frac{1}{5} \frac{1}{m_{\tilde{e}}}$
$\tilde{\gamma}$	$\gamma + \tilde{G}$	$7\times10^{-16} (\frac{M_s}{M_W})^4 \frac{1}{5} \frac{1}{m_{\tilde{\gamma}}}$
$\tilde{q}$	$q + \tilde{g}$	$2\times10^{-23} \frac{m^3_{\tilde{q}}}{(m^2_{\tilde{q}} - m^2_{\tilde{g}})^2} 2$ (in limit $m_q = 0$)
$\tilde{q}$	$q + \tilde{\gamma}$	$3\times10^{-22} \frac{m^3_{\tilde{q}}}{(m^2_{\tilde{q}} - m^2_{\tilde{\gamma}})^2} 2$ (in limit $m_q = 0$).
	$q + \tilde{G}$	$7\times10^{-16} (\frac{M_s}{M_W})^4 \frac{1}{5} \frac{1}{m_{\tilde{q}}}$ (in limit $m_q = 0$)
	$q + \tilde{W}$	roughly the same as $q + \tilde{\gamma}$
$\tilde{g}$	$\tilde{q} + q$	$4\times10^{-23} \frac{m^3_{\tilde{g}}}{(m^2_{\tilde{g}} - m^2_{\tilde{q}})^2}$
$\tilde{g}$	$q + \bar{q} + \tilde{\gamma}$	$10^{-11} (\frac{m_{\tilde{q}}}{M_W})^4 \frac{1}{5} \frac{1}{m_{\tilde{g}}}$ ($m_{\tilde{q}}$ is light-est squark)
$\tilde{g}$	$g + \tilde{G}$	$4\times10^{-16} (\frac{M_s}{M_W})^4 \frac{1}{5} \frac{1}{m_{\tilde{g}}}$
W,Z	$q + \tilde{q}$ $e + \tilde{e}$ etc.	typical of e–m decay. model dependent.

* Here M_s is defined so that the energy density in the vacuum $\langle 0|V|0 \rangle = M_s^4$.

One final comment concerning gaugino masses. The gauginos are Majorana particles, they cannot obtain a Dirac mass unless they combine with some other particles. In the case of $\tilde{W}$ and $\tilde{Z}$ such particles are readily available; they are the Higgsinos. It is possible for the gluinos to obtain a Dirac mass only if there is another set of color octet fermions for them to combine with. The cross section for producing gluinos depends upon whether they are Dirac or Majorana. Since models in which they have a Dirac mass are less popular, they are assumed to be Majorana throughout.

We will now review some of the constraints on models from existing phenomenology. In the limit of exact supersymmetry, (g - 2) for the muon is identically zero.[1.19] The experimental value of (g - 2) puts a limit on $\tilde{\mu}$ and $\tilde{\gamma}$. The contributing Feynman diagrams are shown in Figure 1.2.

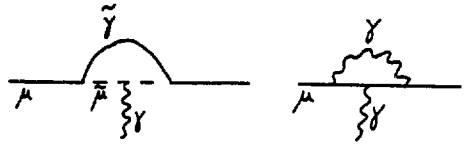

Figure 1.2

In the limit $m_{\tilde{\gamma}} = 0$ and $m_{\tilde{\mu}_L} = m_{\tilde{\mu}_R}$ we have $m_{\tilde{\mu}} \gtrsim 15$ GeV.[1.20] Giving the photino a significant mass barely affects this limit unless there is appreciable mixing between μ_L and μ_R. This mixing is naturally small in models of types two and three.

In models of type three, it is natural that $\tilde{e}_L$ and $\tilde{e}_R$ are not degenerate; this will lead to parity violation in atomic physics and an additional contribution to the parity violation observed at SLAC in ed scattering (Fig. 1.3(a)).

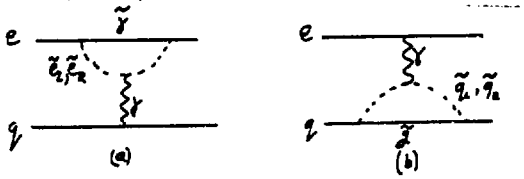

Figure 1.3

The appropriate limit is.

$$\frac{1}{m^2_{\tilde{e}_L}} - \frac{1}{m^2_{\tilde{e}_R}} \lesssim 10^{-2}\ \text{GeV}^{-2}$$

In the case of squarks the limit from ed scattering (Fig. 1.3(b)), is better since α_s enters the correction instead of α_{em}.

$$\frac{1}{m^2_{\tilde{q}_L}} - \frac{1}{m^2_{\tilde{q}_R}} \lesssim 10^{-3}\text{GeV}^{-2}$$

This limit is not as stringent as that from the failure to observe parity violation in nuclei.[1.21] The relevant graphs are shown in Fig. 1.4.

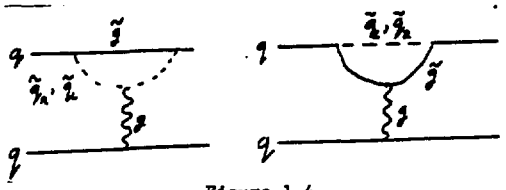

Figure 1.4

Defining $A(u,L) = \dfrac{\log(m^2_{\tilde{u}_L}/m^2_{\tilde{g}})}{m^2_{\tilde{u}_L}}$

we have $A(u,L) - A(u,R) - A(d,L) + A(d,R) \lesssim 3\times10^{-5}\text{GeV}^{-2}$ and $A(u,L) - A(u,R) + A(d,L) - A(d,R) \lesssim 2\times10^{-4}\text{GeV}^{-2}$. These contraints are easily satisfied in models of types two and three. There are also constraints from flavor changing neutral currents. There are two classes of diagrams contributing to the $K_L - K_S$ mass difference. Those diagrams involving wino exchange (Fig. 1.5) give a constraint on the masses of squarks of different flavors, labelled by i.

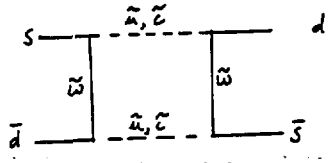

Figure 1.5

If one assumes that the mixing (Cabibbo) angles for squarks are the same as those for quarks, that $m_{\tilde{W}}$ is 100 GeV and that the diagram (Fig. 1.5) is pure imaginary.

$$\frac{m_i^2 - m_j^2}{m_i^2} < 10^{-3}$$

thus all flavors must be about degenerate in mass.[1.22] It is also possible to get a contribution from gluino exchange,[1.23] but only if there is flavor mixing in the squark sector. Models of types two and three naturally satisfy any constraints from flavor changing neutral currents.

Finally there are a number of cosmological constraints on supersymmetric models. There are attempts to constrain the value of $M_{\tilde{g}}$ from the effects of supersymmetric particles on the standard cosmology.[1.24] Taken at face value they exclude a range $10^5 - 10^{12}$ GeV for $M_{\tilde{g}}$. A small value of $M_{\tilde{g}}$ is preferred if one wishes to use gravitinos to explain the missing mass in galaxies.[1.25] Unfortunately almost all models have some cosmological problems with baryon production in the early universe.

In the rest of this report we will concentrate on the partners of known particles, but one should be aware of the extra particles predicted by many models.

References

1.1. J. Wess and B. Zumino, Phy. Lett. 49B, 52 (1974).
1.2. J. Wess and B. Zumino, Phys. Lett. 66B, 361(1977).
1.3. H. M. Georgi and G. L. Glashow, Phys. Rev. Lett. 32, 438 (1974).
1.4. H. Georgi and A. Pais, Phys. Rev. D10, (1974) 539 and references (2-8) therein.
G.'t Hooft, Lecture at Cargese Summer Inst., 1979,

in Recent developments in gauge theories, ed. G. 't Hooft et al., (Plenum, 1980).
1.5. J. Wess and B. Zumino, Phys. Lett. 49B, 52 (1974);
J. Iliopoulos and B. Zumino, Nucl. Phys. B76, 310 (1974);
S. Ferrara, J. Iliopoulos and B. Zumino, Nucl. Phys. B77, 413 (1974).
1.6. S. Deser and B. Zumino, Phys. Rev. Lett. 38, 1433 (1977).
1.7. S. Weinberg, Phys. Rev. Lett. 19, 1264; (1967)
A. Salam, in Elementary Particle Theory, ed. W. Svarthölm (Almqvist and Wikse, Stockholm, 1968) p. 367.
1.8. See the report by W. Marciano (these proceedings).
1.9. S. Dimopoulos and H. Georgi, Nucl. Phys. B193, 150 (1981).
N. Sakai, Z. Phys. C11, 153 (1982).
1.10. R. Barbiera, S. Ferrara, C. A. Savoy, CERN TH 3365 (1982).
1.11. P. Fayet, XVI Rencontre de Moriond, First Session.
1.12. Y. Kang, LBL-14656 (1982);
P. Fayet, Phys. Lett. 95B, 285 (1980); 96B, 83 (1980).
1.13. L. Hall and I. Hinchliffe, Phys. Lett. 112B, 351 (1982).
1.14. L. Alvarez-Gaumé, M. Claudson and M. B. Wise HUTP-81/A063.
1.15. M. Dine and W. Fischler, Phys. Lett. 110B, 227 (1982).
1.16. J. Ellis, L. Ibanez, and G. G. Ross, Phys. Lett. 113B, 283 (1982).
1.17. M. Dine, W. Fischler and M. Srednicki, Nucl. Phys. B189, 575 (1981).
S. Raby and S. Dimopoulos, Nucl. Phys. B192, 353 (1981).
1.18. E. Witten "Constraints on Supersymmetry Breaking", Princeton preprint (1982).
1.19. S. Ferrara and E. Remiddi, Phys. Lett. 84B, 416 (1979).
1.20. P. Fayet, Phys. Lett. 84B, 416 (1979).
1.21. M. Suzuki, Phys. Lett. B115, 40 (1982).
1.22. J. Ellis and D. V. Nanopoulos, Phys. Lett. 110B, 44 (1982).
1.23. M. Suzuki, UCB-PTH-8219 (1982).
1.24. M. Suzuki and P. Q. Hung, (to appear in Phys. Lett.)
S. Weinberg, Phys. Rev. Lett. 48, 1303 (1982).
1.25. J. Primack and H. Pagels, Phys. Rev. Lett. 48, 223 (1982).

II. Proton decay and supersymmetry

In a supersymmetric grand unified theory, there are processes which can contribute to nucleon decay, and which are absent in conventional grand unified theories. In the latter, nucleon decay can be mediated either by heavy ($O(10^{14})$GeV) vector meson exchange (X,Y) or by heavy Higgs exchange (H). For example in the SU(5) model,[1.3] the graphs of Fig. 2.1 give rise to a four-fermion interaction involving quarks (q) and leptons (ℓ) of the form

$$\frac{g^2}{M_X^2}\, qqq\ell \quad \text{or} \quad \frac{g^2}{M_H^2}\left(\frac{m_q}{M_W}\right)^2 qqq\ell \qquad (2.1)$$

where the extra factor of $(\frac{m_q}{M_W})$ arises from the Higgs-fermion coupling. In a supersymmetric theory, there are baryon number violating processes involving squarks.[2.1]

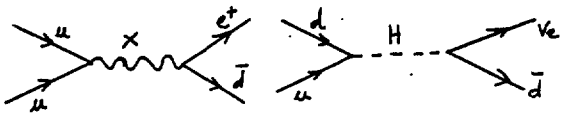

Figure 2.1

The graphs of Fig. 2.2 involving Higgsino exchange give effective interactions of the form

$$\frac{m_q}{M_W}\left(\frac{m_q}{M_W}\right)^2 \frac{1}{M_H}\,(\tilde{q}\tilde{q}q\ell)$$

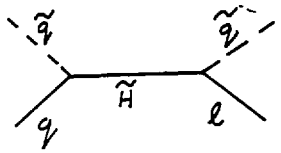

Figure 2.2

If we now couple to quarks via a wino interaction (Fig. 2.3) we have a baryon violating four-fermion interaction

$$\frac{1}{M_H}\frac{1}{M_{\tilde{W}}}\, g^4\left(\frac{m_q}{M_W}\right)^2 (qqq\ell). \qquad (2.2)$$

This contribution is potentially much larger that of (2.1) since $M_{\tilde{W}}$ is much less than M_X in most models

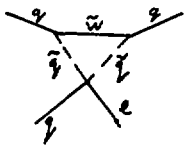

Figure 2.3

(typically $M_{\tilde{W}} \leq 1$ TeV). The exchange of the fermion partners of X and Y does not yield interactions of the form $\frac{1}{M_X}$, but rather $\frac{1}{M_X^2}$ so they are of the same order as 2.1. It appears that 2.2 would lead to a prediction for the proton lifetime which is too short. However, a careful analysis[2.2] in the simplest SU(5) supersymmetric model[1.9] reveals that the rate from 2.2 is roughly the same as that from 2.1 in standard SU(5).[2.3] The reasons for this are the inhibition caused by the $\frac{m_q}{M_W}$ factors, and the increase of the unification scale (hence M_X or M_H) in supersymmetric SU(5) relative to standard SU(5). This increase is caused by the extra particles (principally the gluinos and winos) affecting the evolution of coupling constants.[2.4] In this simple minimal supersymmetric SU(5) the nucleon has a lifetime $O(10^{31})$ years but its decay is principally to $K\nu_\tau$, since the $\frac{m_q}{M_W}$ factors preferentially cause a coupling to the heaviest generation possible.

This conclusion that $p \to K\,\nu_\tau$ is the dominant mode is unfortunately premature. It is possible to construct

models in which 2.2 is suppressed. This can be done either by selecting parameters[2.5] or by a symmetry which forbids the appearance of such terms.[2.1] The latter case occurs naturally in models of type two where the extra U(1) symmetry can be used to eliminate 2.2. In this case the decay $p \to \pi e$ will dominate as in standard SU(5). Unfortunately it is impossible to make a definite statement concerning proton decay. If $p \to K\nu$ dominates then supersymmetry is probably in, if $p \to \pi e$ dominates then models of type two are probably favored if supersymmetry is correct.

References

2.1. S. Weinberg, HUTP 81/A067.
2.2. J. Ellis, D. V. Nanopoulos and S. Rudaz, CERN TH 3199.
2.3. L. Hall, Nucl. Phys. B178, (1981) 75; T. Goldman and D. A. Ross, Phys. Lett. 84B, (1979) 208.
2.4. M. Einhorn and D. R. T. Jones, Phys. Rev. D.
2.5. S. Dimopoulos and S. Raby, LA UR 82/12 (1982).

III. Production of Supersymmetric Particles In $e\bar{e}$ Annihilation

Since squarks and sleptons have the same coupling to the photon and the Z^0 as do quarks and leptons, their production rates in $e\bar{e}$ are easy to estimate, provided there are no extra Z's as are required in models of type two. We will ignore these extra Z's in quoting rates but the readers should be fully aware that the formulae given below are model dependent; they are valid in models of type two only if $M_{Z_{extra}} \gg \sqrt{s}$.

If we ignore $\tilde{e}$ for the moment, asymptotically the production rate is 1/2 of that for the lepton or quark of the same flavor. They are produced via s channel photon and Z exchanges. Figure 3.1(a)

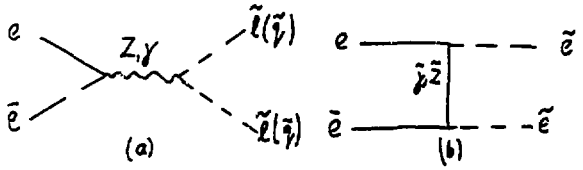

Figure 3.1

the production rates have a β^3 dependence characteristic of scalar particles and a $\sin^2\theta$ angular distribution. The total cross-section is

$$\frac{\pi\alpha^2}{3s} K\beta^3[Q_1^2 - 2\chi Q_1 p(1 - 4\sin^2\theta_W) + p^2\chi^2(1 + (1 - 4\sin^2\theta_W)^2)]$$

where β is the velocity of the squark (slepton) and K = 3 for squarks and K = 1 for sleptons of charge Q_i

$\chi \equiv \left(\frac{s}{s - M_Z^2}\right)\frac{1}{16\cos^2\theta_W\sin^2\theta_W}$. For left handed squarks and sleptons $p = 4Q_i\sin^2\theta_W - 4I_3$ and for right handed $p = 4Q_i\sin^2\theta_W$, with $I_3 = +1/2$ for sneutrinos and charge 2/3 squarks and $-1/2$ for charged sleptons and charge $-1/3$ squarks. In the case of the selectron there are three additional diagrams involving t channel, photino, zino Goldstino exchange,[3.1] Figure 3.1(b). These diagrams are more model dependent since the Goldstino couplings and the masses are not known. Near threshold they will not affect the rate a great deal but asymptotically they are capable of producing large cross sections if the photino mass is very much less than $\sqrt{s}$. The angular distribution is also affected; one obtains the forward peaking characteristic of t channel diagrams. If we ignore the s channel Z and t channel zino the cross-section becomes[3.1]

$$\frac{d\sigma(e\bar{e} \to \tilde{e}_L\bar{\tilde{e}}_L)}{d(\cos\theta)} = \frac{\pi\alpha^2\beta^3\sin^2\theta}{8s}\left[1 + \left(1 - \frac{4}{1 - 2\beta\cos\theta + \beta^2}\right)^2\right]$$

is the approximation that $m_{\tilde{\gamma}} = 0$ and Goldstino graph is negligible. The rate for $\tilde{e}_R + \bar{\tilde{e}}_R$ is of course the same. The rates for $\tilde{e}$ and $\tilde{q}$ are therefore a few(1/2-2) units of R. If they can be pair produced on the Z or any other Z' there will be enough events to detect them. Asymptotically at $\sqrt{s} \approx 750$ GeV a unit of R is of order 15 events per day at a luminosity of 10^{33} $cm^{-2}sec^{-1}$. It is with stressing that in most models (types 2, 3) all flavors are approximately degenerate and the cross-section is correspondingly increased.

We now discuss the signatures. A slepton will decay into the corresponding lepton plus a photino or Goldstino. It is unlikely that $\tilde{\gamma}$ or $\tilde{G}$ will decay within the detector,† so the signature for a slepton pair event is two acoplanar leptons of the same flavor plus missing energy and missing p_t.* The backgrounds are from a heavy lepton, W pairs and two photon events. Most of these are dealt with elsewhere in these proceedings. The first gives a different dependence on p_t of the observed lepton but most importantly will give $e\mu$ pairs at almost the same rate as ee or $\mu\mu$. Slepton decay will never give μe. The W pair background is of course only relevant at very large values of $\sqrt{s}$. Both W's must decay leptonically ($< 1\%$ of events survive this cut) in order to give a background. An angular cut will also help to reduce this since the W cross section peaks near the beam pipe.[3.3] The two photon background can be controlled by requiring that the missing momentum point into the detector.[3.4]

Detecting charged sleptons appears to be no problem, the neutral ones are far more difficult. They are produced due to Z contribution but the decays $\tilde{\nu} \to \nu\tilde{\gamma}$ and $\tilde{\nu} \to \nu\tilde{G}$ produce nothing observable. If $m_{\tilde{\nu}} < m_Z/2$ their presence will enlarge the Z width $\Gamma(Z \to \tilde{\nu}_R\bar{\tilde{\nu}}_R + \tilde{\nu}_L\bar{\tilde{\nu}}_L) = 80\beta^3$ MeV for each generation assuming that $\tilde{\nu}_L$ and $\tilde{\nu}_R$ are degenerate.

If $m_{\tilde{e}} > \sqrt{s}/2$ it may still be possible to observe it.[3.5] The process $e\bar{e} \to \tilde{e}\bar{\tilde{e}}\gamma$ proceeds via the graphs of Fig. 3.2. The total rate $\sigma(M)$ (for $\tilde{e}_L$ or $\tilde{e}_R$) is given by

$$\frac{\sigma(M)}{\sigma_{point}} = \frac{\alpha}{12\pi}\ln\frac{E}{m}\left(\frac{2}{x} + 18 - 54x + 34x^2 + 3(3 - 3x - 4x^2)\ln x - 9x\ln^2 x\right)$$

where $\sigma_{point} = \frac{\pi\alpha}{3E^2}$, E is the beam energy, m is the electron mass and $x = m_{\tilde{e}}^2/4E^2$. Rates are very small, $O(10^{-4})$ units of R for $m_{\tilde{e}} = 1.25$ E; but the signature of one electron at large p_t from the $\tilde{e}$ decay plus

*A search of this type was done by the CELLO group[3.2] at PETRA they quote $m_{\tilde{\gamma}}$, $m_{\tilde{e}}$, $m_{\tilde{e}} \gtrsim 15$ GeV.
†If it does, the event will also have γ's.

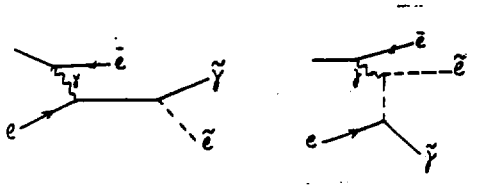

Figure 3.2

missing p_t is very clear. The method has recently been used by the Mark II group at PEP to conclude $m_{\tilde{e}} > 19.5$ GeV.[3.6]

We now turn to squark production. Assuming the gluino is lighter than the squark the decay chain will be $\tilde{q} \to q + \tilde{g}$ ↘ $q\bar{q}\tilde{\gamma}$ or $g\tilde{G}$.

It is unlikely that either the $\tilde{q}$ or $\tilde{g}$ will live long enough to leave a track. On the average 1/6 (1/4) of the squark's energy will be unobserved, carried off by $\tilde{\gamma}(\tilde{G})$. The classic searches for a heavy flavor such as steps in R or increases in sphericity will work in searching for squarks. But the β^3 factor and asymptotic step of 1/2 (assuming q_L and q_R degenerate) relative to a quark of the same flavor will make life hard. (Of course if all flavors are degenerate this is no problem.) It may be possible to exploit the missing energy by only looking at events with some missing energy (and no charged leptons which would result from semi-leptonic decays of heavy flavor). If the gluino is much lighter than the squark then the final state from $(q\bar{q}\tilde{g}\tilde{g})$ will have a four jet structure, and this will help. It is probably possible to detect steps of 1/2 unit of R in the total cross-section,[3.7] so that squarks with mass $\lesssim .3\sqrt{s}$ should be detected. Far above the threshold the $\sin^2\theta$ distribution of jet pairs will confirm that the candidates are indeed scalars.

Squarkonia will be useless as a signal. The 1^{--} bound states which couple to $e\bar{e}$ in the s channel are p wave bound states. The coupling to $e\bar{e}$ of such a state is typically of order 1% of that of an s wave quarkonium of the same flavor. Searches at SPEAR were probably not sensitive to such small effects, it therefore appears that this is not a useful method. The s wave squarkonia can be produced via 2 photon annihilation, but of course only a fraction of $\sqrt{s}$ is available. No observation of the production of η_c in 2 photons at PEP or PETRA has been reported so it seems safe to assume that this method is limited to $m_{\tilde{q}} \lesssim \sqrt{s}/20$.

The only other SUSY particle which couple directly to $e\bar{e}$ are the winos, extra charged Higgs and Higgsinos The charged Higgs cross-sections are discussed elsewhere.[1.8] The winos can be produced pairwise via the diagrams of Fig. 3.3. The sneutrino mass is not known.

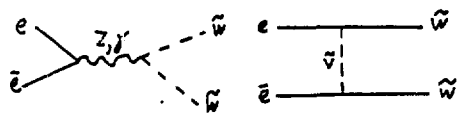

Figure 3.3

Unless $\sqrt{s} \gg m_{\tilde{\nu}}$ the total rate is of the same order as that for smuon production. The exact value also depends on whether or not the wino is a Majorana or Dirac particle. A suitable signal, provided there are enough events is to look for the $\tilde{e}\bar{\nu}$ decay mode (~5% BR) which results in a final state of e^+, e^- and missing momentum (also states of $2e^+2e^-$ from zino pairs). The model dependence of both production cross sections and decay rates makes it difficult to make a more detailed analysis.

Looking for gluinos in $e\bar{e}$ annihilation will be very difficult since they do not couple directly to $e\bar{e}$. We will first discuss processes where gluinos are produced without accompanying squarks. The graphs of Fig. 3.4 result in final states consisting of two quarks and two gluinos.

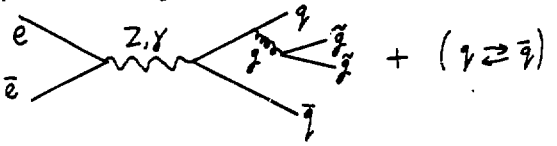

Figure 3.4

The rate is order $(\frac{\alpha_s}{\pi})^2$ compared with $q\bar{q}$ two jet events and consequently will be of order 10^{-2} units of R. It therefore appears that this process will not be of much use in the continuum. However on the Z^0 there may be enough events to be useful. Figure 3.5 shows the ratio $R_1 = \frac{\Gamma(Z \to q\bar{q}\tilde{g}\tilde{g})}{\Gamma(Z \to q\bar{q})}$ as a function of $2m_{\tilde{g}}/\sqrt{s}$.*

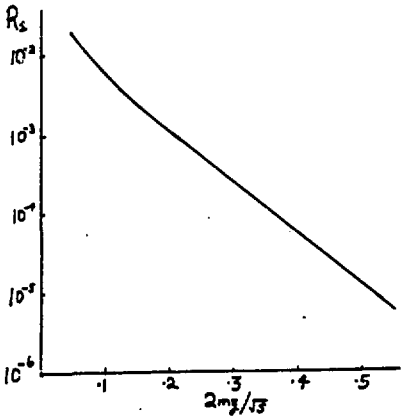

Figure 3.5

The ratio $\frac{\sigma(e\bar{e} \to q\bar{q}\tilde{g}\tilde{g})}{\sigma(e\bar{e} \to q\bar{q})}$ in the continuum will be similar; being almost independent of $\sqrt{s}$ at fixed $m_{\tilde{g}}/\sqrt{s}$ provided $m_{\tilde{g}}/\sqrt{s}$ is not too small. A value of 2×10^{-4} for R_1 corresponds to about 100 events per day on the Z^0 at a luminosity of 10^{32} cm^{-2}sec^{-1}. This corresponds to a gluino mass of 15 GeV. Unfortunately there is a lot of background. A method would be to impose sphericity and acoplanarity cuts to reduce the two and three jet background. A background from four jet event still exists and a cut on missing energy and/or p_t will be required. (Recall that in

* The rates can be obtained from Eq. 5 of Ref. 38) and are valid provided log $m_{\tilde{g}}/\sqrt{s}$ is not too large.

gluino decay energy is carried off by $\tilde{\gamma}$ or $\tilde{G}$). A detailed Monte Carlo simulation is required to settle the question.

Onia have also been suggested as a possible source of gluinos.[3.9] The $^3S_1$ onia (eg ψ or Υ) could decay into two gluons and two gluinos (Fig. 3.6(a))

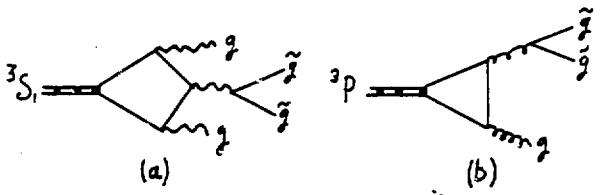

Figure 3.6

$R_2 = \dfrac{\Gamma(^3S_1 \to \tilde{g}\tilde{g}gg)}{\Gamma(^3S_1 \to ggg)}$ is shown in figure 3.7 as a function

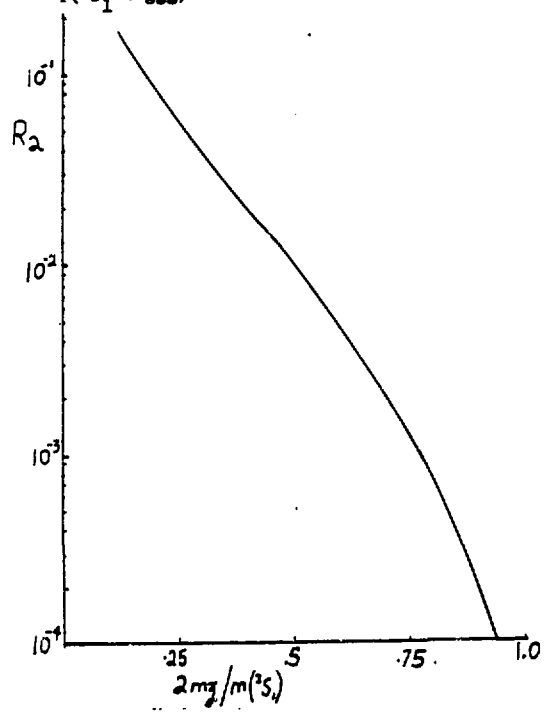

Figure 3.7

of $2m_{\tilde{g}}/m(^3S_1)$. The rates are small. Presumably these events are more spherical than the 3 gluon decay so that a sphericity cut can be used. Unfortunately this is not likely to be effective on the upsilon since the three jet structure of the 3 gluon mode is not very pronounced. Missing energy cuts can be employed and a detailed Monte Carlo simulation including detector details is required but this method does not look very promising. A larger rate can be obtained on the $^3P_1$ state (Fig. 3.b(b))

$$R_3 = \frac{\Gamma(^3P_1 \to \tilde{g}\tilde{g}g)}{\Gamma(^3P_1 \to q\bar{q}g + \tilde{g}\tilde{g}g)}$$

R_3 is of order 0.3 for $2m_{\tilde{g}}/\sqrt{s} \lesssim .8$. Relevent ratios for other P wave states are of the same order.[3.9] Even with such large values it is not clear that enough events can be obtained. Gluinos can also be produced in association with squarks. At very high energy there will be three jet events of the type $e\bar{e} \to \tilde{q}\bar{q}g$. These will have a different angular distribution from the usual $q\bar{q}g$ three jet structure. The graphs of Figure 3.8 produce the $\tilde{q}\bar{q}g$ final state. Defining $x_i = 2E_i/\sqrt{s}$ we have the following event shape for $\tilde{q}\bar{q}g$ in the limit where masses are neglected

$$\frac{d\sigma}{dx_{\tilde{q}}dx_{\bar{q}}} \propto \frac{-1 + x_{\tilde{q}} - 2x_{\tilde{q}}x_{\bar{q}} + 4x_{\bar{q}} - 2x_{\bar{q}}^2}{(1 - x_{\tilde{q}})\ (1 - x_{\bar{q}})}$$

as distinct from the usual form for $q\bar{q}g$.

$$\frac{d\sigma}{dx_q dx_{\bar{q}}} \propto \frac{x_q^2 + x_{\bar{q}}^2}{(1 - x_q)\ (1 - x_{\bar{q}})}$$

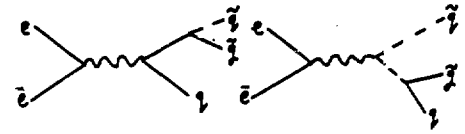

Figure 3.8

At lower values of $\sqrt{s}$ where masses cannot be neglected the formulae are much more complicated.[3.10] For simplicity we will concentrate on the Z^0. The ratio $R_4 = A\dfrac{\Gamma(Z \to q_i\tilde{q}_i\tilde{g})}{\Gamma(Z \to q_i\bar{q}_i)}$ is shown in Figure 3.9. Here

$$A \equiv \frac{4(1 + (4Q_i\sin^2\theta_W - 2I_3)^2)}{p^2}.$$

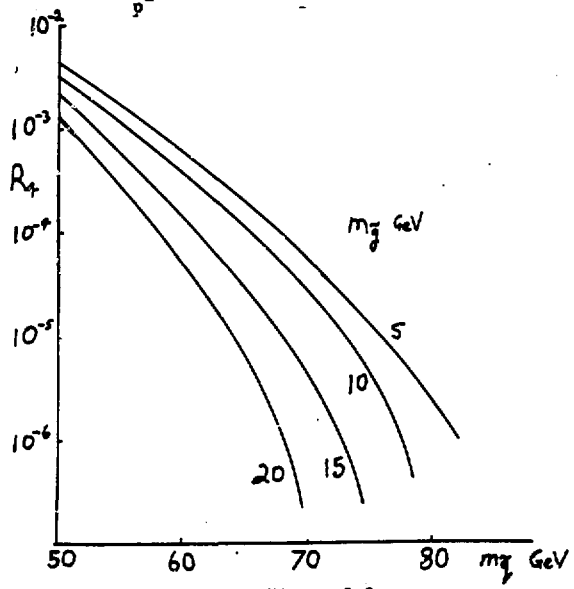

Figure 3.9

Of course the rate is larger if $\sqrt{s} > 2m_{\tilde{q}}$ since the (on shell) squarks can then decay to $\tilde{g}q$. R_4 is shown only in the more interesting case $\sqrt{s} < 2m_{\tilde{q}}$. Experimentally we would use a combination of sphericity and missing energy cuts to dig out the signal.

References

3.1. P. Fayet and G. Farrar Phys. Lett. 89B, 191 (1980).
3.2. Cello collaboration, H. T. Behrend, et al., DESY 82/021 (1982).
3.3. I. Hinchliffe, these proceedings.
3.4. See the discussion in 3.7.

3.5. M. K. Gaillard, L. Hall and I. Hinchliffe, Phys. Lett. (to appear).
3.6. W. Chinowsky, private communication to I. H.
3.7. See the report of the High energy $e\bar{e}$ group in these proceedings.
3.8. G. C. Branco, H. P. Willes and K. H. Streng, Phys. Lett. 85B, 269 (1979).
3.9. B. A. Campbell, J. Ellis, S. Rudaz, Nucl. Phys. B198, 1 (1982).
3.10. I. Hinchliffe in preparation.

IV. Production in ep

If the gluino is much lighter than the squark there are two possible ways in which its presence could be detected in ep collisions. In the absence of gluinos and squarks, asymptotically the fraction of the proton's momentum carried by quarks as revealed by deep inelastic scattering is $\frac{3N_f}{16 + 3N_f}$ where N_f is the number of flavors. The rest of the momentum is of course carried by gluons. If gluinos and squarks exist they will affect this fraction. If squarks are light enough to be excited their presence will be indicated by a change in $F_2(x, Q^2)$ since they couple to weak and electromagnetic interactions. Gluinos will reveal their presence indirectly by carrying some fraction of the proton's momentum. If Q^2 is large enough so that gluinos contribute but squarks do not, the momentum fraction carried by quarks becomes $\frac{3N_f}{20 + 3N_f}$.[3.9] The change from 52% to 47% (for $N_f = 6$) is not very large, and since the approach to asymptotic is rather slow, this does not look like a very promising method to search for gluinos.

Gluinos can be produced in pairs either in charged current or neutral current processes (Fig. 4.1)

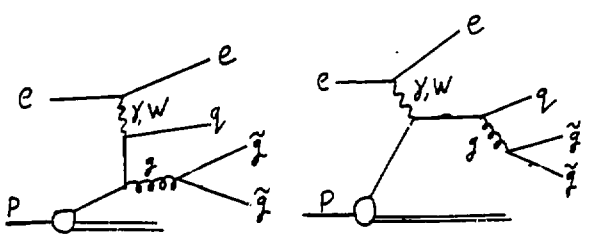

Figure 4.1

The ratios

$$R^{CC} \equiv \frac{\sigma(ep \to \nu\tilde{g}\tilde{g}X)}{\sigma(ep \to \nu X)} \quad \text{and} \quad R^{NC} = \frac{\frac{d\sigma}{dxdy}(ep \to e\tilde{g}\tilde{g}X)}{\frac{d\sigma}{dxdy}(ep \to eX)}$$

are shown in Fig. 4.2 as a function of $s/4m_{\tilde{g}}^2$.[3.9] According to the notes by T. O'Halloran,[4.1] a 10 GeV electron on 1 TeV proton machine will produce $O(10^5)$ charged current events for an integrated luminosity of 10^{39} cm^{-2}. It therefore appears that there are unlikely to be sufficent events for this process to be useful given that the signature is not very clear. Unless the gluino is kind enough to leave a track, cuts on missing energy and p_t will be required (the method is the same as that discussed in the next section).

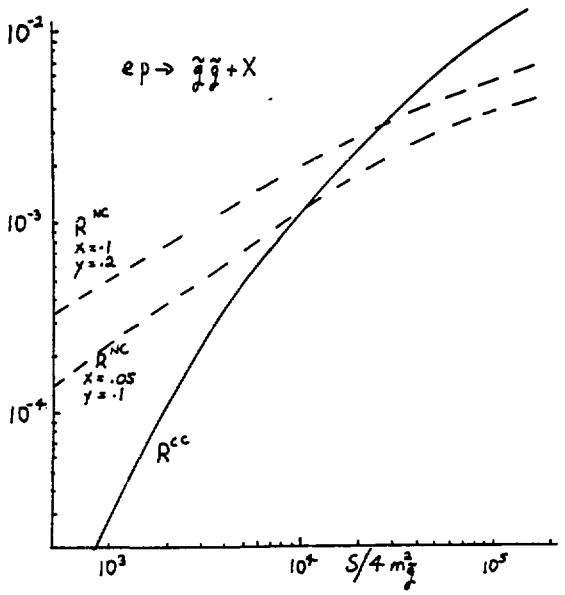

Figure 4.2

A more promising process in ep collisions is the production of a squark and a selectron via the graph of Fig. 4.3.

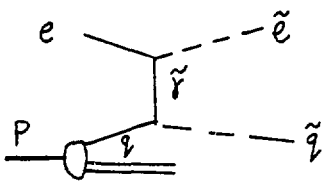

Figure 4.3

The invariant cross section

$$e(\text{momentum } k) + q(q) \to \tilde{e}_L(k') + \tilde{q}_L(p)$$

can be written as follows (J. Leveille and I. H.)

$$\frac{d\sigma}{du} = \frac{\pi Q_i^2 \alpha^2}{s^2(t + m_{\tilde{e}}^2)^2}[ut + m_{\tilde{q}}^2 t + m_{\tilde{e}}^2 u] \qquad (4.1)$$

where

$$s = 2k\cdot p, \quad t = -2k\cdot k', \quad u = -2k\cdot p.$$

The photino mass has been neglected, it is unlikely to affect the rates quoted below provided it is not heavier than about 20 GeV. There are of course additional graphs involving zino and wino exchange but they are not included in this estimate. Those involving wino exchange have larger couplings (since $g_{weak} > e$) but produce $\tilde{\nu}\tilde{q}$ final states. Integrating 4.1 using the parton distributions of Ref. 4.2 yield the rates shown in Figure 4.4 for an intergrated luminosity of 10^{39} cm^{-2}.* We have assumed that $\tilde{q}_i$ are degenerate in mass for up, down, and strange flavors and have performed a flavor sum. We have not summed over $\tilde{e}_L$ and $\tilde{e}_R$. Of course the rates for $\tilde{e}_L$ and $\tilde{e}_R$ are the same if they are degenerate in mass. The signature for these events is

* $\sqrt{s}$ = 200 GeV corresponds to 10 GeV electron on 1 TeV protons, $\sqrt{s}$ = 319 GeV to 30 GeV electrons and 800 GeV protons and $\sqrt{s}$ = 2830 GeV to 100 GeV electrons and 20 TeV protons.

an electron (from $\tilde{e}$ decay) plus missing energy and p_t, carried off by $\tilde{\gamma}$ or $\tilde{G}$. Rates are large and this mechanism looks promising.

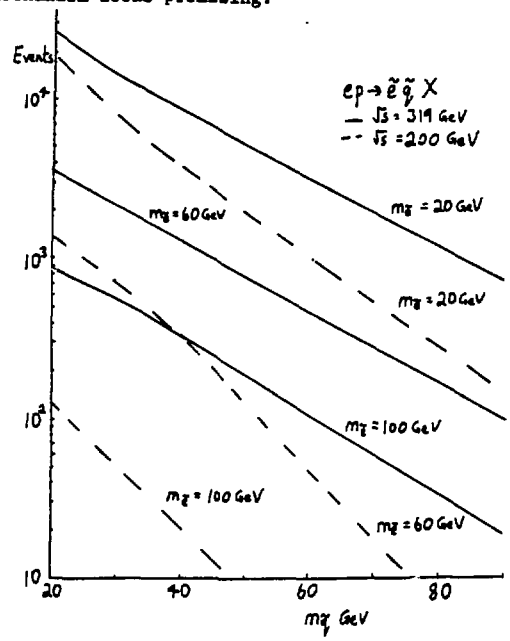

Figure 4.4

Squarks can be produced in pairs using the photon gluon fusion mechanism.[4.3] The cross section

$\gamma(q) + g(p) \to \tilde{q}_L(p') + \bar{\tilde{q}}_L(q')$ is [J. Leveille]

$$\frac{d\sigma}{du} = \frac{\alpha_s \alpha Q_i^2 \pi}{s^2} \left[1 - \frac{2m_{\tilde{q}}^2 s}{tu} + \frac{2m_{\tilde{q}}^4 s^2}{u^2 t^2}\right]$$

with $s = 2p\cdot q$, $t = -2q\cdot p'$ $u = -2q\cdot q'$, and Q_i is the squark charge. The rates are shown in Fig. 4.5; the value shown is σ/Q_i^2 and is per flavor and per chirality state; again 10^{39} cm^{-2} has been assumed for an integrated luminosity [Figure due to J. Wiss]

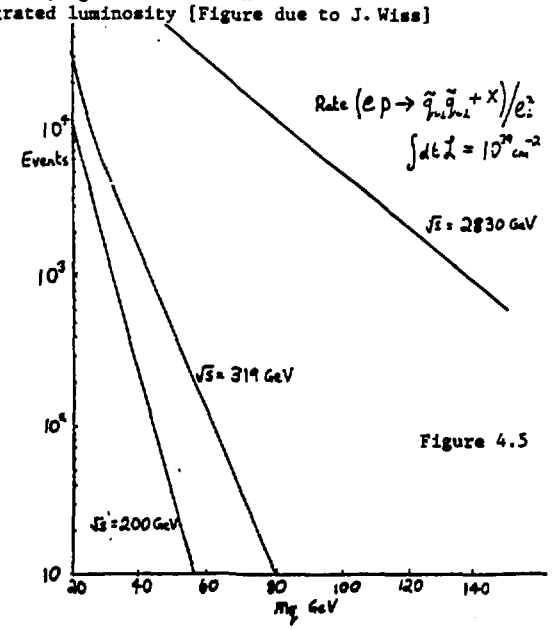

Figure 4.5

Squarks may also be photo-produced in ep collisions the graphs of Fig. 4.6 yield for the cross section $\gamma(q) + q(p) \to \tilde{q}_L(p') + \tilde{g}(q')$. [J. Leveille and I. H.]

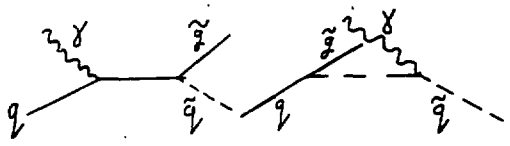

Figure 4.6

$$\frac{d\sigma}{du} = \frac{4\pi\alpha\alpha_s Q_i^2}{3s^2}\left[\frac{u}{s} - \frac{2m_{\tilde{q}}^2}{t^2}\left[t^2 + m_{\tilde{q}}^2 - m_{\tilde{g}}^2\right]\right.$$

$$\left. + \frac{\left[(u-t)(m_{\tilde{q}}^2 - m_{\tilde{g}}^2) + s^2(m_{\tilde{q}}^2 + m_{\tilde{g}}^2) - 2(m_{\tilde{q}}^2 - m_{\tilde{g}}^2)^2\right]}{st}\right] \quad (4.2)$$

where $u = -2q\cdot q'$ $s = 2p\cdot q$ $t = -2q\cdot p'$ and Q_i is the quark charge. The cross section for $\tilde{q}_R$ is of course the same. Using the Weizacher Williams[4.4] approximation the rate for $\tilde{q}_L$ is shown in Fig. 4.7. (u,d,s flavors summed, again $\int dt\mathcal{L} = 10^{39}$). In the case that the gluino is too heavy to be produced, the process $\gamma q \to \tilde{q}\tilde{\gamma}$ may be observed. The cross section is that given in 4.2 multiplied by $\frac{3Q_i^2}{4}\frac{\alpha}{\alpha_s}$ with $m_{\tilde{g}} = m_{\tilde{\gamma}}$.

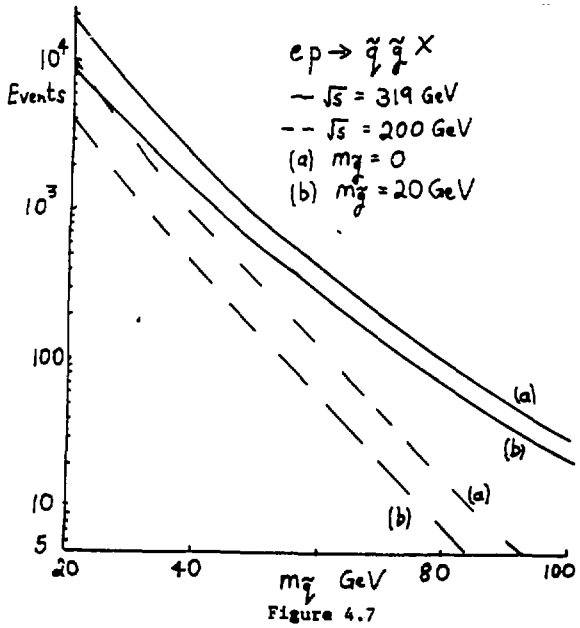

Figure 4.7

Reference

4.1. See the report of the lepton hadron collider group.

4.2. R. Baier, et al., Z. Phys. C2, 259 (1978).

4.3. J. P. Leveille and T. Weiler, Nucl. Phys., B147, 1147 (1974)

4.4. C. Weizacher and E. T. Williams, Z. Physik, 88, 612 (1934).

V. Production of Supersymmetric Particles at Hadron-Hadron Colliders

As mentioned in Section I, once the masses of squarks and gluinos are chosen, the interactions of these particles with normal quarks and gluons are completely determined. Thus it is straightforward to calculate their production cross-section in pp or $p\bar{p}$ collisions via QCD perturbation theory.[5.1] Such calculations should be subject to no more uncertainty than e.g., the analogous calculations of heavy quark production cross-sections.* The leading diagrams for gluinos, shown in Figure 5.1, have been calculated by J. Leveille to give:

a) gluon fusion

$$\frac{d\sigma}{dt} = \frac{\pi\alpha_S^2}{32\,s^2}\ \frac{1}{2}\left\{\left(\frac{u}{t}+\frac{t}{u}\right)\ C_1(1+\gamma) - 2(C_1 - C_2) + 2C_2\gamma + \frac{4ut}{s^2}\ (C_1 - C_2) - 4m_{\tilde{g}}^4\ C_1\left(\frac{1}{t^2}+\frac{1}{u^2}\right) - 8m_{\tilde{g}}^4 C_2\ \frac{1}{ut}\right\}$$

b) quark-antiquark fusion

$$\frac{d\sigma}{dt} = \frac{\pi\alpha_S^2}{9\,s^4}\ \frac{1}{2}\ \ C_3\ [2m_{\tilde{g}}^2 s + t^2 + u^2]$$

where $s = (k_1 + k_2)^2$ The k's are the initial and the p's the final parton 4-momenta

$t = -2k_1\cdot p_1$

$u = -2k_1\cdot p_2$

$\gamma = \frac{4m_{\tilde{g}}^2}{s}$

$C_1 = 72$ $\quad C_1' = 16/3$

$C_2 = 36$ $\quad C_2' = -2/3$

$C_3 = 24$

Figure 5.2 shows the results for $\sigma(pp \to \tilde{g}\tilde{g}X)$ at $\sqrt{s}$ = 0.06, 0.54, 0.80, 2, 10, and 40 TeV.† It should be noted that these cross-sections are relatively large, typically 5 to 10 times corresponding cross-section for production of normal (fermionic) heavy quarks. Thus if a suitably distinctive signature for such events can be found, one can hope to probe gluino masses up to a substantial fraction of $\sqrt{s}/2$.

*Where they can be checked, these calculations tend to underestimate the observed cross-sections by a factor 2 or more, so that estimates for supersymmetric particle production made in this way can presumably be regarded as conservative.[5.2]

†Constituent cross-sections supplied by J. Leveille have been integrated using a special version of the ISAJET[5.3] program. We assume that $\tilde{q}_L$ and $\tilde{q}_R$ are degenerate. The Baier structure functions and Λ = .1 GeV are assumed. Since these cross-sections are dominated by the contribution of gluon-gluon fusion, the corresponding $\bar{p}p$ cross-sections are rather similar.

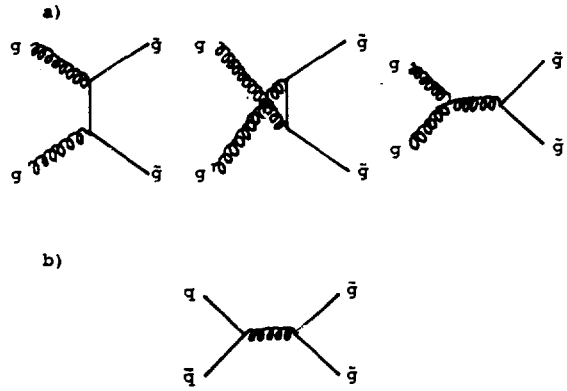

Figure 5.1. a) Gluino pair production via gluon-gluon fusion. b) Gluino pair production via quark-antiquark fusion.

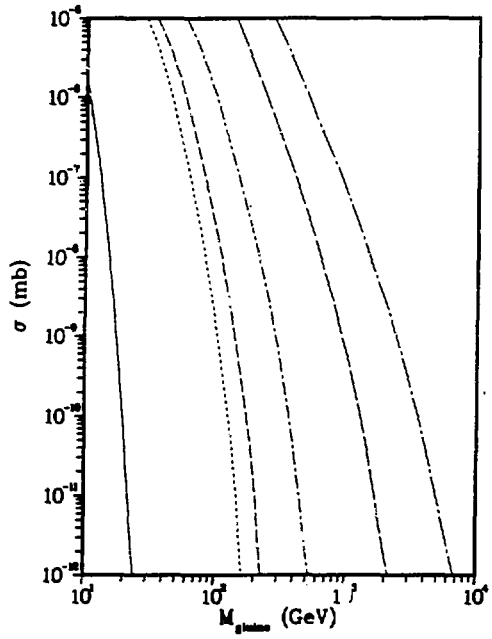

Figure 5.2. Production cross-sections for the reaction $pp \to \tilde{g}\tilde{g}X$ as a function of $m_{\tilde{g}}$. From left curves are for $\sqrt{s}$ = .06, .54, .80, 2.0, 10.0, and 40.0 TeV.

The same mechanisms which produce gluino pairs can also produce squark antisquark pairs. However, here spin and color factors reduce the cross-section by a factor $\sim$ 50 with respect to that for gluino pairs. A much more copious source of scalar quarks is provided by the diagrams of Figure 5.3 in which the squarks are produced in association with gluinos.¶ The parton level cross-sections, also calculated by J. Leveille are:

¶To a good approximation this process produces only $\tilde{u}$ and $\tilde{d}$.

$$\frac{d\sigma}{dt} = \frac{\pi\alpha_S^2}{24\,s^2}\;2\;\frac{(s^2+t^2)\,C_1' + 2stC_2'}{s^2t^2u^2}$$

$$\times \{-ust^2 + 2ust(m_{\tilde{g}}^2 - m_q^2)$$

$$- 2us(m_{\tilde{g}}^2 - m_q^2) - 2S\,m_{\tilde{g}}^2(m_{\tilde{g}}^2 - m_q^2)\}$$

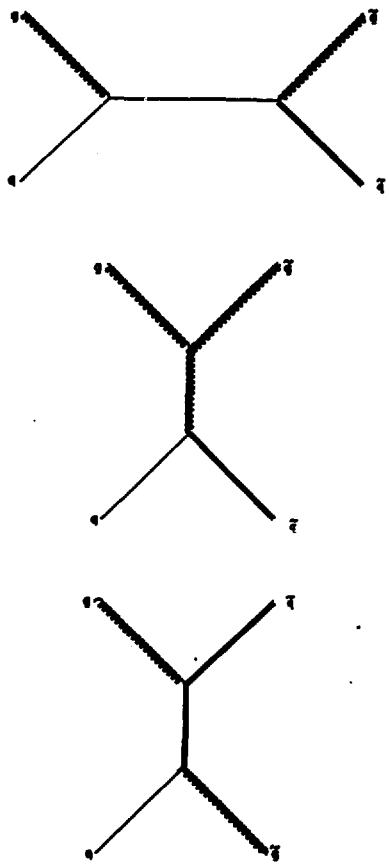

Figure 5.3. Quark + gluon goes to squark + gluino.

Here one is helped enormously by the possibility of making the squark off a valence quark, and in the case of a relatively light gluino, by the fact that the penalty for making a heavy particle need only be paid once. Cross-sections for two cases of interest are shown in Figures 5.4 and 5.5. Figure 5.4 shows the cross-section for $pp \to \tilde{g}\tilde{q}X$ in the case that $m_{\tilde{g}} = m_{\tilde{q}}$. This is meant to represent the predictions of type three models in which these masses tend to be comparable. Note that over most of the range of m and $\sqrt{s}$ covered here, the $\tilde{q}\tilde{g}$ cross-section is 3 to 5 times higher than the corresponding $\tilde{g}\tilde{g}$ cross-section. Since, as will be discussed below, the signatures of gluino pair and of (equal mass) $\tilde{q}\tilde{g}$ events are very similar, if $m_{\tilde{g}} \gtrsim m_{\tilde{q}}$ the latter process would be the more accessible to observation.

In models of type two, $m_{\tilde{g}}/m_{\tilde{q}}$ is more likely to be near α_s than 1. In this case the gluino will probably be observed first via its production in pairs, leaving the squarks to be discovered somewhat later in associated $\tilde{g}\tilde{q}$ production at higher energies. Figure 5.5 shows the cross-sections relevant to this case. Here $m_{\tilde{g}}$ has been set to 10% of $m_{\tilde{q}}$. These cross-sections are very large indeed, about two orders of magnitude larger than those of the equal mass case.

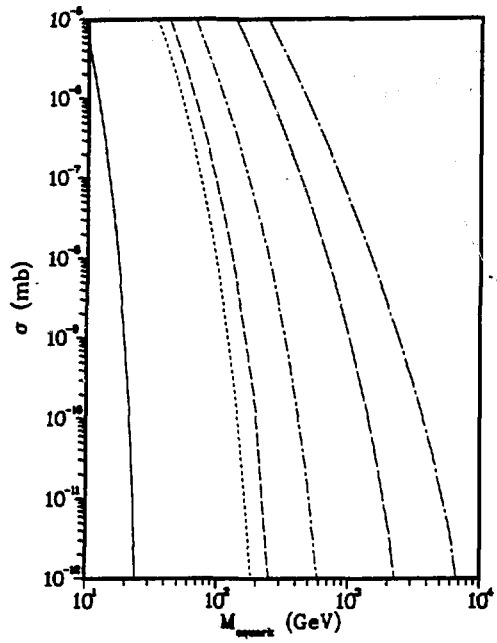

Figure 5.4. Production cross-sections for the reaction $pp \to \tilde{g}\tilde{q}X$ as a function of $m_{\tilde{q}}$. It is assumed that $m_{\tilde{g}} = m_{\tilde{q}}$. From left curves are for $\sqrt{s}$ = .06, .54, .80, 2.0, 10.0, and 40.0 TeV.

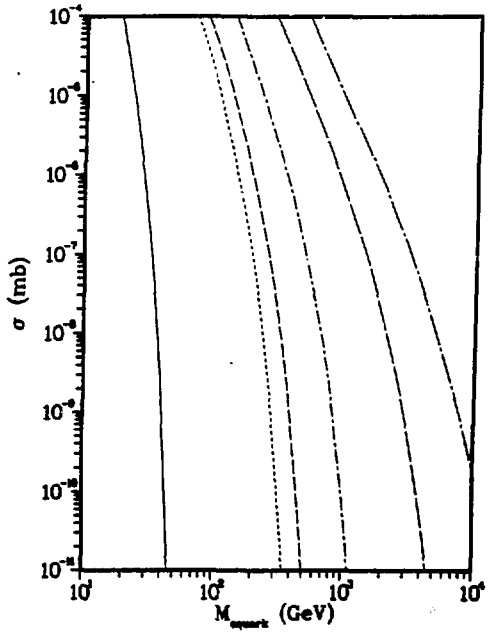

Figure 5.5. Production cross-section for the reaction $pp \to \tilde{g}\tilde{q}X$ as a function of $m_{\tilde{q}}$. It is assumed that $m_{\tilde{g}} = 0.1\ m_{\tilde{q}}$. From left curves are for $\sqrt{s}$ = .06, .54, .80, 2.0, 10.0, and 40.0 TeV.

To make a really complete assessment of the possible signatures for supersymmetric hadron production one needs to know the masses (particularly the relative masses) of the various particles, and also the scale of supersymmetry breaking, M_S. However, as shown by the work of Aronson, et al.,[5.4] even without this knowledge certain general conclusions can be drawn that survive in most reasonable scenarios. As discussed in Sections II and III, the supersymmetric hadron partners decay directly or via a rapidly evolving sequence of decays into some combination of quarks, antiquarks and gluons and one long lived, relatively weakly interacting supersymmetric particle (e.g., a photino). The g's, $\bar{q}$'s and g's materialize into jets of hadrons while the SUSY particle normally eludes the detector.* Such events will appear to have missing energy and unbalanced momentum. Since events containing heavy quarks which decay semileptonically also display this property, the signature can be further improved by demanding the absence of high p_T leptons.

The example of gluino pair production has been given the most attention. If the gluino is lighter than the lightest squark it will decay into gluon + Goldstino at a rate, $\Gamma_G = 2.4 \times 10^{15} \left(\frac{M_W}{M_S}\right)^4 \left(\frac{m_{\tilde{g}}}{1\ \text{GeV}}\right)^5 \text{sec}^{-1}$. It can also decay into a photino + a quark antiquark pair at a rate $\Gamma_{\tilde{\gamma}} = 10^{11} \left(\frac{m_{\tilde{g}}}{1\ \text{GeV}}\right)^5 \left(\frac{M_W}{m_{\tilde{q}}}\right)^4 \text{sec}^{-1}$ $10^{11} \left(\frac{M_W}{m_{\tilde{q}}}\right)^4 \left(\frac{m_{\tilde{g}}}{1\ \text{GeV}}\right)^5 \text{sec}^{-1}$ (where $m_{\tilde{q}}$ represents the lightest squark mass). Thus if $M_{\tilde{q}} \lesssim .1\ M_S$, the photino decay dominates. In any case, for the range of masses being considered here, $\Gamma_{\tilde{\gamma}}$ is large enough to render the gluino flight path unobservably short. The gluino pair production cross-sections rise to a broad peak at around $p_T \sim m_{\tilde{g}}/2$ and then fall off roughly exponentially in E_T, giving $\langle p_T \rangle \sim m_{\tilde{g}}$. Thus, even after the escape of the photino or Goldstino there tends to be a loosely collimated jet of hadrons with reasonably high $\sum \vec{p}_T$ on each side of the beam. The loss of the light particles however ensures that the residual jets will not balance p_T. The undetected particles carry off energy as well, but it is very difficult to exploit this property since accurate measurements of the fast particles near the beams would be required.

To illustrate how a p_T imbalance signature could be utilized, we outline the study of Reference 5.4. In that work signal (and background) events emanating from pp collisions at $\sqrt{s}$ = 800 GeV were generated using the ISAJET[5.3] Monte Carlo program and subjected to a simulated detector. This detector was based on a fine-grained, high resolution uranium calorimeter covering the full range in azimuth and rapidity - 2 < y < 2. Charged particle tracking and lepton identification over the range - 3 < y < 3 was also assumed. Visible p_T of at least 20 GeV/c on one side of the beam and of at least 5 GeV/c on the opposite side was demanded. It was found convenient to characterize the degree of p_T imbalance by means of the variables $x_E = -\vec{p}_T \cdot \vec{p}'_T / |\vec{p}_T|^2$ and $P_{out} = \sqrt{|\vec{p}'_T|^2 - x_E^2 |\vec{p}_T|^2}$ where $\vec{p}_T$ denotes the larger and $\vec{p}'_T$ the smaller $\sum \vec{p}_T$ of the two residual jets. The distributions of these quantities for $m_{\tilde{g}}$ = 30 and 75 GeV are shown in Figures 5.6 and 5.7. It is assumed that $\tilde{g} \to \bar{\gamma}\bar{q}q$, briefly, the x_E distributions are roughly triangular, peaking near 1; $\gtrsim$ 20% of events have $x_E < .5$. The shape of this distribution is a rather weak function of gluino mass. By contrast, the P_{out} distribution vary nearly scales in $P_{out}/m_{\tilde{g}}$. It falls fairly gently from $P_{out} = 0$, reaching 50% of its initial height at $\sim m_{\tilde{g}}/6$, and 10% at $\sim m_{\tilde{g}}/3$. Shown for comparision are the x_E and P_{out} distributions of light constituent (u,s,d,g) scattering which dominates the trigger rate at high p_T. Not surprisingly these distributions peak sharply at $x_E = 1$ and $P_{out} = 0$. At the present summer study, the work of Reference 5.4 was extended to higher values of s, and it was found that the shapes of both signal and background distributions changed extremely slowly with energy. It was also found, somewhat surprisingly, that the gluino distributions do not depend strongly on the gluino decay mode: results for the case $\tilde{g} \to G\tilde{g}$ were significantly, but not strikingly, different from those of $\tilde{g} \to \bar{\gamma}\bar{q}q$. For example when $\tilde{g} \to \bar{\gamma}\bar{q}q$ ($M_{\tilde{g}}$ = 75 GeV/c^2, $\sqrt{s}$ = 800 GeV), 20% of the gluino events passed the cuts $x_E < .5$, $P_{out} > 5$ GeV/c, whereas when $\tilde{g} \to G\tilde{g}$, 27% of the events passed these cuts. Since the three body case gives slightly more pessimistic results, it is used in most of the estimates given herein.

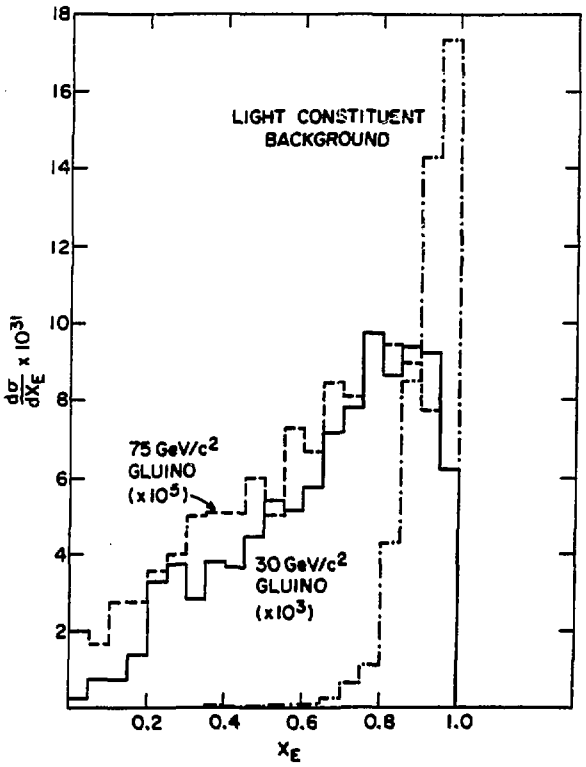

Figure 5.6. X_E distributions for gluino pair production at $\sqrt{s}$ = 800 GeV. Also shown is the corresponding distribution for light constituent scattering. (From Ref. 5.4).

*Certainly it eludes a hadron-hadron collider detector. In principle at a fixed target machine it is possible to observe these particles in, for example, a neutrino detector. Such a strategy has already been used to place limits on various SUSY masses, lifetimes etc. (See Ref. 5.1 and Section VI).

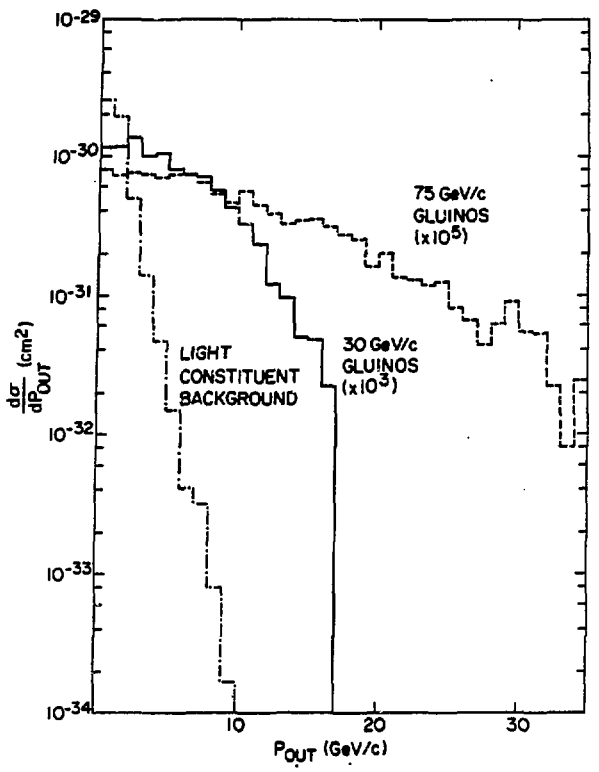

Figure 5.7. P_{out} distributions for gluino pair production at $\sqrt{s}$ = 800 GeV. Also shown is the corresponding distribution for light constituent scattering. (From Ref. 5.4).

In the process $pp \to \tilde{g}\bar{q}X$, in general the signature depends on both $m_{\tilde{g}}$ and $m_{\tilde{q}}$.* However, for our limiting case of $m_{\tilde{g}} \gtrsim m_{\tilde{q}}$, when $m_{\tilde{q}}$ is assumed to decay to $\tilde{g}q$, and $\tilde{g}$ to $\bar{\gamma}\bar{q}q$, it is found that the x_E and p_T distributions are virtually identical to those of gluino pair production at the same mass. Thus it appears that for equal mass SUSY particle production, while there is a slight degradation of the p_T signature as the number of partons in the final state increases from two to four, there is no further change as this number is increased to five. However, when one of the masses is made much lighter than the other, as in our second limiting case ($m_{\tilde{g}} = 0.1\ m_{\tilde{q}}$), the signature is significantly compromised. Both the x_E and p_T distributions are affected. Table 5.1 gives the results of comparison between the equal mass case $m_{\tilde{g}} = m_{\tilde{q}} = 50$ GeV/c^2 and the unequal mass case $m_{\tilde{g}} = 10$ GeV/c^2, $m_{\tilde{q}} = 100$ GeV/c^2 ($\sqrt{s}$ = 800 GeV). It should be noted that in this example the superior cross section of the unequal mass case more than compensates for its inferior signature.

If $m_{\tilde{g}} > m_{\tilde{q}}$ as in at least one type three model,[1.16] the gluino decay chain will presumably be $\tilde{g} \to \bar{q}\tilde{q} \to \bar{q}q\tilde{\gamma}$, i.e., the same final state will be produced as in the direct three body decay. The signature for gluino pair production will then be nearly identical to the one discussed above. The signature of associated $\tilde{g}\tilde{q}$ production is likely to be marginally better than those discussed above for the $M_{\tilde{q}} \gtrsim M_{\tilde{g}}$ and $M_{\tilde{q}} >> M_{\tilde{g}}$ cases, since in most scenarios there will be one or two fewer partons in the final state. The cross sections for this case have not yet been calculated; they are probably comparable to the corresponding cross-sections with $m_{\tilde{q}}$ and $m_{\tilde{g}}$ reversed. The signature for $\tilde{q}\bar{q}$ production will also be improved; the 'visible' final state will include only two high p_T partons.

We will now discuss the backgrounds. At the trigger level, the leading background is high p_T light constituent scattering. For the detector discussed above, at $\sqrt{s}$ = 800 this process would give $\sim$ 500 events/sec with $p_T > 20$ GeV/c for $\mathcal{L} = 10^{32}$ cm^{-2} sec^{-1}. Clearly one would need to implement some sort of p_T-imbalance trigger on-line. A 50-fold reduction in trigger rate seems quite practicable. In any case a p_T threshold as low as 20 GeV/c is only necessary for the lowest values of $m_{\tilde{g}}$ that would be probed at such a facility whereas the signal event rates for these masses are so large (e.g., one gluino pair/sec for $m_{\tilde{g}}$ = 30 GeV/c^2) that a ten-fold prescaling of the trigger would be quite acceptable.

Offline, once cuts on P_{out} and x_E have been imposed, (with effects on the signal as described above) the light constituent background is reduced by factors of $\lesssim 10^4$. The identity of the leading residual background then becomes a matter for detailed Monte Carlo study. Four types of background were considered in the context of the detector of Ref. 5.4: (1) high p_T light constituent scattering, (2) high p_T production of $t\bar{t}$ pairs, (3) high p_T production of $b\bar{b}$ and $c\bar{c}$ pairs, (4) W production, followed by $W \to \tau\nu_\tau$. The dominant residual background proves to be a pernicious component of background (1) in which a high p_T gluon fragments into a high mass $b\bar{b}$ or $c\bar{c}$ pair. If one of the heavy quarks then decays semileptonically, the momentum transverse to the parent gluon carried away by the ν can be quite considerable, typically $\sim p_T/6$. Such an event can simulate the p_T-imbalance signature. At $\sqrt{s}$ = 800, this background amounts to 0.5 - 5.0 $\times 10^{-34}$ cm^2, depending on the choice of cuts. Since the degree of p_T imbalance in this process does not depend strongly upon the flavor of the heavy quark, it is fair to ask whether in fact strange quarks, too, can contribute. This is of course a much more apparatus dependent question. For the detector under discussion, where the flight paths are a meter or two, the contribution of strange quarks turns out to be < 10% of that of heavier flavors.

Background 2), $t\bar{t}$ production, can also manifest p_T imbalance in the case of a semi-leptonic decay. Here the missing p_T with respect to the t jet-axis is $\sim m_t/3$ The degree of p_T imbalance obviously increases with increasing t quark mass, but the production cross-section decreases. It should be remembered that for equal masses, the gluino pair cross-section will be 5 to 10 times higher than the $t\bar{t}$. Assuming m_t = 20 GeV/c^2, at $\sqrt{s}$ = 800 GeV this background can contribute a few times 10^{-35} cm^2 after p_T imbalance cuts.

The cross-section for direct $b\bar{b}$ and $c\bar{c}$ production is several times higher than that for $t\bar{t}$ for $p_T > 20$ GeV/c (Assuming m_t = 20 GeV/c^2). This is found to be completely offset by the smaller p_T imbalance; the residual contribution of background (3) is approximately one order of magnitude less than that of the $t\bar{t}$ pairs.

After p_T-imbalance cuts are imposed, background (4) yields a residual cross-section of $\sim 10^{-35}$ cm^2 at $\sqrt{s}$ = 800 GeV. However these events differ in many respects from typical gluino pair events. Most of the cross-section stems from low p_T W production so that the recoil "jet" is rather soft and tends to be composed of many individually low p_T particles. The higher p_T "jet" is actually the visible product of the τ decay and is, therefore, highly collimated and of extremely low multiplicity when compared to gluino jets. Cuts can be devised which reduce this background to a negligible level, without significantly depleting the

*The $\tilde{q}$ decay rates given in Section I ensure that the $\tilde{q}$ decay path is unobservably short.

supersymmetric particle production signal.

Thus we find that all significant residual backgrounds are associated with leptons, most often muons or electrons. Even when the leading lepton is a tau, a muon or electron will frequently be present either from semileptonic decays further down the chain of sequential heavy flavor decay, or from the decay of the τ itself. This phenomenon will be crucial to the convincing extraction of the supersymmetric particl signal. If, as seems likely, it is possible to tag electronic or muonic events with $p_T^{LEPT} \gtrsim 2$ GeV/c, one can achieve reductions in the total background by a factor of 3 or more. Equally important, the measured properties of the identified leptonic events should greatly facilitate the calculation of the number of background events in which the leptons go undetected. Such calculations which would be extremely difficult to get right without the benchmark provided by the identified leptonic events should become sufficiently reliable that a SUSY signal can be extracted from an equal or even somewhat larger background.

During the summer study the background calculations were extended to the case of $\bar{p}p$ collisions at $\sqrt{s}$ = 2 TeV. Roughly speaking the backgrounds increased by about the same factor as did the signals.

The extraction of the gluino pair signal at $\sqrt{s}$ = 800 GeV is discussed in detail in Reference 5.4. A luminosity of 10^{32} cm^{-2} sec^{-1} was assumed, which seems sufficiently conservative, in light of the work of Gordon et al.[5.5] To decide whether even higher luminosity could be used requires a more detailed study with a more realistic detector simulation program. The situation at $\mathcal{L} = 10^{32}$ cm^{-2} sec^{-1} is summarized by Figure 6 of Reference 5.4 which shows the $p_T^{visible}$ distribution for various mass gluinos and for the background after the cuts have been imposed. It seems clear that one could extract a gluino pair signal for $m_{\tilde{g}} \geq 100$ GeV/c^2. Assuming a 10^7 second run, for $m_{\tilde{g}} = 100$ GeV/c^2 one would have about 2500 signal events with $p_T^{visible} > 65$ GeV/c compared with a residual background of 1500 events in the same kinematic region. For the case of a 2 TeV $\bar{p}p$ collider with $\int \mathcal{L} dt = 10^{36}$, a similar criterion gives a gluino mass limit of $m_{\tilde{g}} \sim 70$ GeV/c^2.

In the case of $\tilde{g} + \tilde{q}$ associated production one does somewhat better. If $m_{\tilde{g}} = m_{\tilde{q}}$ the signature is very similar to that of gluino pairs and the cross-section is approximately three times higher. In this case masses of ~ 125 GeV/c^2 seem quite accessible for $\sqrt{s}$ = 800, $\int \mathcal{L} dt = 10^{39}$. Similarly for $\bar{p}p$ interactions at 2 TeV, M $\sim$ 100 should be attainable at $\int \mathcal{L} dt = 10^{36}$. Although the detailed Monte Carlo study for the case $m_{\tilde{q}} >> m_{\tilde{g}}$ has not yet been completed, preliminary indications are that truly impressive values of $m_{\tilde{q}}$ can be probed. Figure 5.8 shows the visible p_T spectrum of $\tilde{g}\tilde{q}$ and background events after cuts for $m_{\tilde{q}} = 200$ GeV/c^2, $m_{\tilde{g}} = 20$ GeV/c^2, $\sqrt{s}$ = 800, $\int \mathcal{L} dt = 10^{39}$. A signal of $\sim$ 30,000 events towers over a small background. It's quite clear that the $m_{\tilde{q}}$ limit could be pushed quite a bit higher, perhaps to 250 GeV/c^2.

TABLE 5.1

	$m_{\tilde{g}}$ = 50 GeV/c^2 $m_{\tilde{q}}$ = 50 GeV/c^2	$m_{\tilde{g}}$ = 10 GeV/c^2 $m_{\tilde{q}}$ = 100 GeV/c^2
σ detected (mb)	1.08×10^{-6}	9.583×10^{-6}
fraction of evts with $x_g < .5$	.27	.13
fraction of cuts with $P_{out} > 5$ GeV/c	.55	.25
fraction of evts passing both cuts	.16	.04

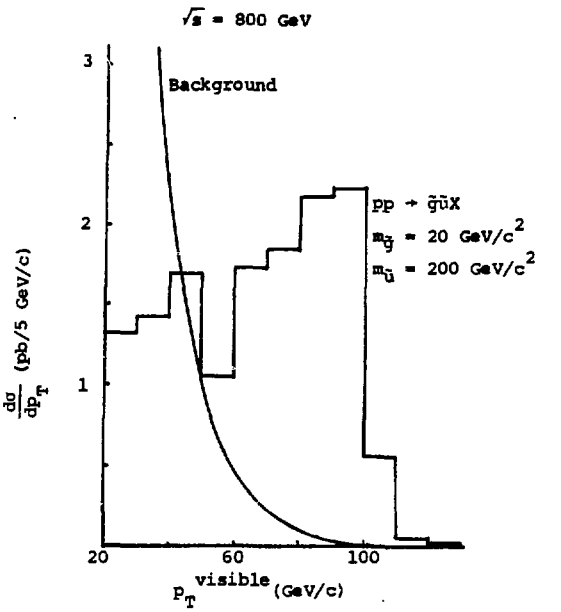

Figure 5.8. Histogram is visible p_T distribution for $p + p \to \tilde{g} + \tilde{u} + X$ at $\sqrt{s}$ = 800 GeV, $m_{\tilde{g}} = 20$ GeV/c^2, $m_{\tilde{q}} = 200$ GeV/c^2. Solid curve is residual background.

References

5.1 G.L. Kane and J.P Leveille, Phys. Lett. 112B, 319 (1982).

5.2 V. Barger, et al., Phys. Rev. D25, 112 (1982).

5.3 F.E. Paige and S.D. Protopopescu, ISAJET: A Monte Carlo Event Generator for pp and $\bar{p}p$ Interactions. These proceedings.

5.4 S.H. Aronson, L.S. Littenberg, F.E. Paige, I. Stumer and D.P. Weygand, "Detecting Supersymmetric Hadrons." These proceedings.

5.5 H.A. Gordon, et al., "Reasons Experiments can be Performed at a pp Machine at L = 10^{33} cm^{-2} sec^{-1}. These proceedings.

VI. Production of Supersymmetric Particles at Fixed Target Hadron Accelerators

Two studies of the production of supersymmetric particles at fixed target machines were conducted by members of this subgroup. The first,[6.1] by R. Lipton assessed the prospects for detecting gluino pair events at a 20 TeV fixed target machine. It was similar to the study described in Section V in that the events were to be detected in a large aperture calorimetric apparatus and identified by momentum imbalance and by the absence of leptons. In addition, the missing energy was to be exploited, something which is very difficult to do in collider experiments. Assuming that in the fixed target case missing energy is identifiable to equivalent luminosities of 10^{33} cm^{-2} sec^{-1}, one can accumulate > 100 gluino pairs for $m_{\tilde{g}} \lesssim 55$ GeV/c^2. Although a detailed Monte Carlo program was not available for this study, an estimate of the background indicated that it would not be the limiting factor.

M. Longo and J. Leveille studied the senaitivity of 20 TeV fixed target beam dump experiments to supersymmetric particles. This work is based on the experience of the Fermilab E613 beam dump experiment.[6.2] Interacting in such a detector, photinos or Goldstinos

resulting from gluino decay would produce events which look like muonless ν events, but with a broader p_T distribution. Three separate cases are considered.* In the first case it is assumed that the gluino decays into $\tilde{\gamma}q\bar{q}$ and that the $\tilde{\gamma}$ is long lived and consequently reaches and interacts in the detector. Assuming the photino interaction cross section is given by[6.3]

$$\sigma_{int}(\tilde{\gamma} \to \tilde{g}) \approx 2 \times 10^{-37} E_{\tilde{\gamma}} \left(\frac{M_W}{m_{\tilde{q}}}\right)^4 \times \left\{ \sum_q \int_x^1 e_q^2 \, d\xi \; \xi q(\xi) \; (1 - \frac{x}{\xi})^2 \; (1 + \frac{x}{8\xi}) \right\} cm^2$$

where $q(\xi)$ is the q quark distribution function, e_q is its charge, and $x \equiv m_{\tilde{g}}^2/s$, for this case E613 finds $m_{\tilde{g}} \gtrsim 5$ GeV/c^2 assuming $m_{\tilde{q}} \approx M_W/2$. A similar experiment at 20 TeV should detect interacting photinos if $m_{\tilde{g}} \lesssim 21$ GeV/c. Note, however, that if $\sqrt{s} > m_{\tilde{q}}$, there is likely to be a large enhancement in the photino cross-section due to photoproduction of squarks off valence quarks. This, order electromagnetic, cross-section could cause the photinos to be absorbed before reaching the detector.

In case 2 it is assumed that $\tilde{g} \to \tilde{G}g$ or that $\tilde{g} \to \tilde{\gamma}q\bar{q}$ and that the $\tilde{\gamma}$ subsequently decays rapidly to a Goldstino. If the $\tilde{G}$ interacts via a Goldstino-gluon fusion mechanism, its cross section in the detector is given by:[5.1]

$$\sigma_{int}(\tilde{G}) \approx \frac{3.7}{M_S} m_{\tilde{g}}^2 (1 - x) \quad mb,$$

where $x = \frac{m_{\tilde{g}}^2}{s}$ as before, and all masses are in GeV units. Clearly the limits obtained depend on both $m_{\tilde{g}}$ and M_s. Table 6.1 gives the results:

TABLE 6.1

E613		20 TeV Experiment	
$m_{\tilde{g}}$	M_s	$m_{\tilde{g}}$	M_s
3 GeV/c^2	$\gtrsim$ 0.5 TeV	12.5	$\gtrsim$ 1.4 TeV
4	0.3	17	$\gtrsim$ 0.8
5	0.2	21	0.5
6	0.12	25	0.3

Case III assumes that $\tilde{g} \to \tilde{\gamma}\bar{q}q$ and that the photino lifetime is long enough that they have a reasonable probability of decay in the detector. It was found that a 20 TeV experiment would easily detect $\tilde{\gamma}$'s if $m_{\tilde{g}} \leq 40$ GeV/c^2.

It should be noted that if the gluino lifetime is sufficiently long for the shadron bearing it to survive even a few centimeters, it will tend to interact before it can decay. This will soften the momentum spectrum of the photinos or Goldstinos which ultimately result to the point where the above searches may be compromised.

Thus it appears that experiments of the former type will be more sensitive, once the energy is high enough for the p_T imbalance trigger to be effective.

Finally we turn to the possibility of finding shadrons by looking for tracks in emulsion or bubble chambers. The lifetime of the lightest shadron (i.e., the one stable in strong interactions) must be greater than 10^{-14} sec for this possibility to arise. If one looks at the table of lifetimes in Section I, the only possibility appears to be a rather light gluino (less than 5 GeV/c^2), if one assumes that $m_{\tilde{q}}$ is not much larger than M_W. We cannot tell a priori whether or not the lightest shadron involving a gluino will have electronic charge (e.g., $\tilde{g}u\bar{d}$) or not (e.g., $\tilde{g}g$). If $m_{\tilde{g}} \gtrsim 2$ GeV, bag model calculations indicate that charged shadrons are stable in strong interactions.[6.4] A charged shadron is, of course, easier to detect than a neutral one. Since momentum and energy are carried off by unobserved particles, the observed particles from the decay of a neutral shadron will not point back to the primary vertex making a search more difficult.

If the shadron lifetime is very long (greater than that of a Λ) than searches for contamination in beams should be able to set limits. The experiment of Ref. 6.5 searched for contamination at FNAL. They looked for particles which traveled .59 kilometers from the production vertex and then interacted with a cross-section of order 1 mb. In the case of neutral particles the limit on the production cross-section ($\sqrt{s}$ = 28 GeV) was 10^{-35} cm^2. Assuming a gluino production cross-section of 20 μb thus translates into a limit on the lifetime; the gluino must live less than about 2×10^{-8} sec for this experiment to have missed it. A similar search in hyperon beams is capable of a stronger limit since the flight path is shorter. We are not aware of any published limits and would encourage an experimentalist to provide one.

If the lifetime is shorter than 10^{-11} sec then the recent searches for charm should have seen something. Here a word of caution is needed, experimentalists often find only what they are looking for, and sometimes fail even to do that.† Some experiments in neutrino beams triggered on external muons and others required a V which pointed back to the vertex. Recently data have become available from high resolution bubble chambers.[6.6] Such chambers were probably sensitive to shadron decay and indeed, an attempt to set a limit was made. A search was conducted looking for two components in the lifetime (one from charm and one from shadrons); no evidence for two components was found. It seems fair to conclude that the production rate at $\sqrt{s} \simeq 20$ GeV is less than a few microbarns, implying that $m_{\tilde{g}}$ is greater than 2-3 GeV, but more work is needed.

References

6.1 R. Lipton, "A Search for Massive Gluinos at a 20 TeV Fixed Target Machine." These proceedings.

6.2 R.C. Ball, et al., "Supersymmetric Mass and Lifetime Limits from a Proton Beam Dump Experiment," University of Michigan Report HE82-21 (1982).

6.3 J. Leveille, private communication, and P. Fayet, Phys. Lett. 86B, 272 (1979).

6.4 M. Chanowitz and S. Sharpe, private communication.

6.5 H.R. Gustafson, et al., Phys. Rev. Lett. 37, 474 (1976), and J. Appel, et al., Phys. Rev. Lett. 32, 428 (1974).

6.6 G. Kalmus "Weak Decays of New Particles," Review talk at Paris Conference.

VII. Conclusion

The theoretical situation with regard to supersymmetry is exceedingly confused. There is a plethora of models most of which are phenomenologically acceptable but differ radically in their predictions of the properties of the as yet undiscovered particles. The next generation of machines will be able to constrain these models severely.

*The interpretation of possible results given here implicitly assumes that $m_{\tilde{q}} >> m_{\tilde{g}}$.

†A number of searches failed to find charm and set limits on the production cross-section an order of magnitude below the currently accepted value.

$e\bar{e}$ machines such as LEP CESRII or SLC should easily be able to discover sleptons up to masses of order $.9E_{beam}$. With slightly more effort squarks up to these masses should also be observable. $e\bar{e}$ machines will have great difficulty discovering gluinos. If the gluino is light ($\lesssim$ 15 GeV) then $Z \to q\bar{q}\tilde{g}\tilde{g}$ will generate 0 (100) events/day. Such a rate may be observable by exploiting missing energy and sphericity cuts. At higher energy 3 jet events from $e\bar{e} \to q\bar{q}\tilde{g}$ which have a different angular distribution than $ee \to q\bar{q}g$ should be observable; but only sufficiently far above the $\tilde{q}\tilde{g}$ threshold for the jet structure to be clear ($\sqrt{s} \gtrsim 10\ (m_{\tilde{q}} + m_{\tilde{g}})$).

ep machines tend to have rather small rates of the pair production of squarks and for the photoproduction of squarks and gluinos and squarks and photinos. The rates of $ep \to \tilde{e}\tilde{q} + X$ are more promising. With reasonable event rates of order 10/day at $L = 10^{32}\ cm^{-2}\ sec^{-1}$, one can reach masses satisfying $(m_{\tilde{q}} + m_{\tilde{g}}) \approx \sqrt{s}/2$. In hadron colliders event rates are very large but backgrounds are serious. By applying cuts on missing p_T, Monte Carlo studies show that all these backgrounds are manageable. A high luminosity pp machines ($L \sim 10^{32}$) should be above to detect gluinos up to a mass of order $\sqrt{s}/7$. If the squark is much heavier than the gluino then the squark cross-section is large and is should be possible to reach squark masses of order $\sqrt{s}/3$. Beam dump studies at fixed target machines may be sensitive to gluino mass of order $\sqrt{s}/7$, but their interpretation is model dependent. Direct searches, using unbalanced p_T and missing energy seem more promising and may allow gluino masses of order $\sqrt{s}/4$ to be reached.

Much work remains to be done in the experimental applications of supersymmetry and we hope that this document will be useful in indicating the status of current ideas.

This work was supported in part by the U.S. Department of Energy under Contract Numbers DE-AC03-76SF00098 and DE-AC02-76CH00016.